Linear Semibridging Carbonyls. 4. A Consequence of Steric Crowding and Strong Metal-to-Metal Bonding

Charles Q. Simpson II and Michael B. Hall*

Contribution from the Department of Chemistry, Texas A&M University, College Station, Texas 77843-3255. *Received July 26, 1991*

Abstract: Ab initio full-gradient geometry optimizations have been performed on 28 of 36 M–M closed-shell electronic configurations for the $M_2(CO)_2$ (M = Sc and Mn) model systems. Those configurations whose energy favors a bridging carbonyl structure always prefer a bent semibridging or symmetrically bridging geometry. Conversely, when the carbonyls, of those configurations whose energy favors terminal carbonyls, are forced into bridging sites, a linear semibridging structure results. *Thus, linear semibridging carbonyls are a consequence of steric crowding.* Generally, those configurations that favor a bent semibridging or symmetrically bridging carbonyl have more metal-to-metal antibonding molecular orbitals occupied (particularly the σ^*). In contrast, those configurations that favor a terminal structure, and hence a linear semibridging carbonyl in sterically crowded molecules, have more metal-to-metal bonding orbitals occupied. *Thus, the appearance of linear semibridging carbonyls signifies strong metal-to-metal bonding.*

Introduction

Since the discovery of bridging carbonyls,[1,2] a number of investigations[3-10] have contributed to our understanding of the interaction between metal atoms and bridging carbonyl ligands. Recently, the various bridging modes—terminal (**1**), bent semibridging (**2**), symmetric bridging (**3**), linear semibridging (**4**), and prone semibridging (**5**)—have been clearly delineated.[3]

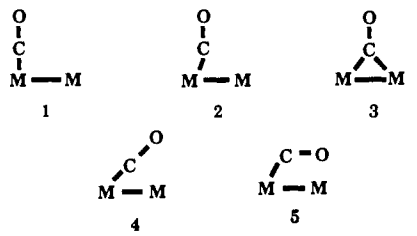

In the first description of the bonding for bent semibridging carbonyls, Cotton proposed that semibridging carbonyls accept electrons from the secondary metal atom in order to equalize the charge difference between the two metals.[4,5] Colton and co-workers prepared the first compound with a linear semibridging carbonyl, $Mn_2(CO)_5(dppe)_2$. Subsequently, Curtis and co-workers found that $Cp_2Mo_2(CO)_4$ also had linear semibridging carbonyls with a Mo–C–O bond angle of 175.9° (1.2).[6] They proposed that linear semibridging carbonyls donate electron density from their 1π orbital to the distal M. In 1980, Colton and McCormick suggested that the structural form that a bridging carbonyl assumes in the solid state is a result of inter- and intramolecular steric forces; they also rationalized several different types of bridging carbonyls using these steric arguments.[7]

In 1980 Hoffmann and co-workers performed extended Huckel calculations on $Cp_2Mo_2(CO)_4$ and $Cp_2Fe_2(CO)_4$, which have four linear semibridging and two symmetrically bridging carbonyls, respectively.[8] Their results suggested that the bridging carbonyl ligand, for each of the cases bent semibridging (**2**), symmetric (**3**), or linear semibridging (**4**), accepts electron density from the metal d orbitals into its 2π orbital, a suggestion consistent with Cotton's original hypothesis. However, they did not offer an explanation for the linearity of some semibridging carbonyls.

Subsequent work by Hall and co-workers on $Cp_2Mo_2(CO)_4$ lent further support to the work of Hoffmann and Cotton, and also offered an explanation for the linearity of the carbonyl ligand.[9a] Benard and co-workers performed ab initio calculations on the $Mn_2(CO)_5(PH_3)_4$ model system and reached similar conclusions.[10] In this description the CO inserts one of the C lobes of its 2π acceptor orbital into an occupied, in-phase combination of metal d orbitals to form a 3-center, 2-electron bond. This interaction can be stabilizing for structure **4** but not for structure **2** or **3**. Recently, Sargent and Hall found that a linear semibridging carbonyl may also donate electron density when the distal metal is an electron deficient early transition metal rather than a late transition metal from which it always accepts electrons.[9b,c]

It is generally agreed that carbonyls bond to metals through both σ and π bonds. In the simplest view, the σ bond is formed when electron density flows from the carbonyl 5σ (lone pair) to an empty metal orbital, and the π bond forms when electron density flows from the filled metal $d\pi$ to the carbonyl 2π. For the symmetric bridging form (**3**), the carbonyl strongly accepts electron density from both metals into its 2π orbitals, a transfer of charge which results in a much weaker CO bond. For the prone semibridging form (**5**), the carbonyl apparently accepts density from the first metal and donates to the distal metal from its 1π orbital or O "lone pair." The nature of the semibridging geometries, **2** and **4**, seems to provoke the most discussion with three explanations vying for prominence. Two focus on the electronic (attractive) interactions. In the first explanation both geometric forms involve the carbonyl accepting electron density from the secondary metal center, where the difference in metal orbital character gives rise to the difference in geometry. The second explanation suggest that in the linear semibridging form, **4**, the carbonyl donates electron density to the second metal. The third explanation focuses on the steric (repulsive) interactions. Here, the electronic interactions with the second metal are thought to be negligible and the observed geometry of the semibridging carbonyl is determined by the steric requirements of the total coordination sphere of the dimer or cluster.

Using a model that is itself free from significant steric effects in the metal coordination environment, we have determined how occupation of different metal–metal orbitals affects the geometry of the bridging carbonyl ligand. We have examined steric effects

(1) Powell, H. M.; Ewens, R. V. G. *J. Chem. Soc. A* **1939**, 286.
(2) Sheline, R. K.; Pitzer, K. S. *J. Am. Chem. Soc.* **1950**, *72*, 1107.
(3) (a) Crabtree, R. H.; Lavin, M. *Inorg. Chem.* **1986**, *25*, 805. (b) Shinn, N. D.; Trenary, M.; McClellan, M. R.; McFeely, F. R. *J. Chem. Phys.* **1981**, *75*, 3142.
(4) Cotton, F. A. *Prog. Inorg. Chem.* **1976**, *21*, 1.
(5) Colton, R.; Commons, C. J.; Hoskins, B. F. *J. Chem. Soc., Chem. Commun.* **1975**, 363.
(6) Klinger, R. J.; Butler, W. M.; Curtis, M. D. *J. Am. Chem. Soc.* **1978**, *100*, 5034.
(7) Colton, R.; McCormick, M. J. *J. Coord. Chem. Rev.* **1980**, *31*, 1.
(8) Jemmis, E. D.; Pinhas, A. R.; Hoffmann, R. *J. Am. Chem. Soc.* **1980**, *102*, 2576.
(9) (a) Part 1: Morris-Sherwood, B. J.; Powell, C. B.; Hall, M. B. *J. Am. Chem. Soc.* **1984**, *106*, 5079. (b) Part 2: Sargent, A. L.; Hall, M. B. *J. Am. Chem. Soc.* **1989**, *111*, 1563. (c) Part 3: Sargent, A. L.; Hall, M. B. *Polyhedron* **1990**, *9*, 1799.
(10) Benard, M.; Dedieu, A.; Nakamura, S. *Nouv. J. Chim.* **1984**, *8*, 149.

0002-7863/92/1514-1641$03.00/0 © 1992 American Chemical Society

by forcing certain geometric distortions on the model system and examining the response of the model.

Theoretical Methods

Models and Basis Sets. In this study the model dimers $M_2(CO)_2$ (M = Sc and Mn) were used. All basis sets for the ab initio calculations were derived from those of Huzinaga.[11] For Sc and Mn we used the double-ζ basis (432/421/31) of previous calculations,[12] and for C and O we used the (321/21) double-ζ basis set.

Calculations. The ab initio molecular orbital (MO) calculations were performed via the closed-shell Hartree–Fock–Roothaan (HFR) method.[13] A series of three ab initio full-gradient geometry optimizations were performed on the M–M electron configurations (vide infra) of the $M_2(CO)_2$ (M = Sc and Mn) model compounds. The M–C and C–O bond distances and M–C–O bond angle (ϕ) were optimized for various choices of configuration and M–M–C bond angle. The M–M bond distance was set equal to 2.220 Å.

The ab initio calculations were performed with the GAMESS[14] program package. Calculations were carried out on the Department of Chemistry VAX 11/780 and FPS 264 processor and the Cornell National Supercomputing Facility's FPS 264 processors and IBM 3090-600J mainframes.

Results and Discussion

Our first objective is to determine if occupation of particular metal–metal (M–M) molecular orbitals (MO) in a system free of steric interferences has any control over the geometry that a bridging carbonyl assumes. Thus, we chose the model system **6**,

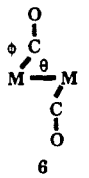

6

which consists of two metal atoms and two symmetry-related bridging carbonyls. Of course, this model is also coordinatively unsaturated at both metal centers, because of the lack of other ligands. Our purpose here is not to determine the true ground-state structure of these $M_2(CO)_2$ molecules but to use these as models for a sterically uncrowded $(L_nM)_2(\mu\text{-}CO)_2$ molecule. As a model for these molecules, we will be most interested in alternative 3d–3d closed-shell electronic configurations.

For $Sc_2(CO)_2$ and $Mn_2(CO)_2$ there are 6 and 14 M–M electrons, respectively, and for each system there are 18 closed-shell possibilities for occupation of the 10 M–M MO's formed from the 3d orbitals shown in Table I. These electronic configurations are labeled so that each number of a four-digit configuration label specifies how many M–M MO's of a particular symmetry are doubly occupied. The order is a_g, a_u, b_g, and b_u. For example, the configuration label 3211 for $Mn_2(CO)_2$ specifies that the configuration would have three doubly occupied a_g orbitals, two doubly occupied a_u orbitals, one doubly occupied b_g orbital, and one doubly occupied b_u orbital. In other words, the M–M electron configuration $1a_g^2$, $2a_g^2$, $3a_g^2$, $1a_u^2$, $2a_u^2$, $1b_g^2$, $1b_u^2$ would be encoded as 3211.

Four configurations (3000 and 0003 for $Sc_2(CO)_2$; 0223 and 3220 $Mn_2(CO)_2$) were omitted because we belived they were high in energy and unrealistic models for real molecules. Four configurations (2100, 1123, 2221, 2122), dissociated during optimization or did not converge in the self-consistent-field (SCF) portion of the calculation, therefore, 15 configurations were studied for $Sc_2(CO)_2$ and 13 for $Mn_2(CO)_2$. For each configuration the M–M–C bond angle (θ) was fixed at 90°, 80°, and 70°. The M–C and C–O bond distances and the M–C–O bond angle (ϕ) were optimized at each value of θ.

Table I. Metal-to-Metal Molecular Orbitals[a]

M-M MO	Type	C_{2h} symmetry
	σ	a_g
	σ^*	b_u
	π_{ip}	b_u
	π_{op}	a_u
	π^*_{ip}	a_g
	π^*_{op}	b_g
	δ_{op}	b_g
	δ_{ip}	a_g
	δ^*_{op}	a_u
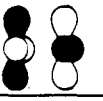	δ^*_{ip}	b_u

Table II. Electron Configuration Labels for the M–M MO's of $M_2(CO)_2$ (M = Sc or Mn)

Sc $a_ga_ub_gb_u$	Mn $a_ga_ub_gb_u$	Sc $a_ga_ub_gb_u$	Mn $a_ga_ub_gb_u$	Sc $a_ga_ub_gb_u$	Mn $a_ga_ub_gb_u$
3000[a]	0223[a]	0201	3022	0012	3211
2100[b]	1123[b]	1020	2203	0003[a]	3220[a]
2010	1213	0120	3103	1110	2113
2001	1222	0021	3202	1101	2122[b]
1200	2023	1002	2221[b]	1011	2212
0210	3013	0102	3121	0111	3112

[a] Omitted. [b] Dissociated or did not converge.

Results for M = Mn. For the $Mn_2(CO)_2$ configurations, the Hartree–Fock–Roothaan (HFR) total energy as a function of θ is shown graphically in Figure 1. As θ decreases some of the $Mn_2(CO)_2$ configurations increase in energy while the others decrease. With few exceptions the $Mn_2(CO)_2$ configurations can be separated into two distinct groups.

Those configurations that increase in energy—3112, 3211, 3121, 3202, 3022, 3013—are illustrated with solid lines. Two of these $Mn_2(CO)_2$ configurations, 3121 and 3202, initially increase but then decrease in energy as θ moves from 80° to 70° (see Figure 1). Those configurations that decrease in energy—2212, 2113, 3103, 2203, 2023, 1222, 1213—are illustrated with dashed lines, and their changes appear to be consistent to 70°. Thus, six configurations favor a terminal carbonyl geometry while seven configurations favor a bridging carbonyl geometry.

Since one can make a clear distinction between those carbonyls which favor a bridging position and those that do not, one might

(11) *Gaussian Basis Sets for Molecular Calculations*; Huzinaga, S., Ed.; Elsevier: Amsterdam, 1984.
(12) Williamson, R. L.; Hall, M. B. *Int. J. Quantum Chem. Symp.* **1987**, *21*, 502.
(13) Roothaan, C. C. *J. Rev. Mod. Phys.* **1951**, *23*, 69.
(14) Guest, M. F.; SERC Daresbury Laboratory, Warrington WA4 4AD, U.K.
(15) Interactive MOPLOT: A package for the interactive display and analysis of molecular wave functions incorporating MOPLOT (Lichtenberger, D.), PLOTDEN (Bader, R. F. W.; Kenworthy, D. J.; Beddall, P. M.; Runtz, G. R.; Anderson, S. G.), SCHUSS (Bader, R. F. W.; Biegler-Koenig, F. W.), and EXTREME (Bader, R. F. W.; Biegler-Koenig, F. W.); Sherwood, P., MacDougall, P. J., 1989.
(16) Simpson, C. Q., II, Ph.D. Dissertation, Texas A&M University, 1991.

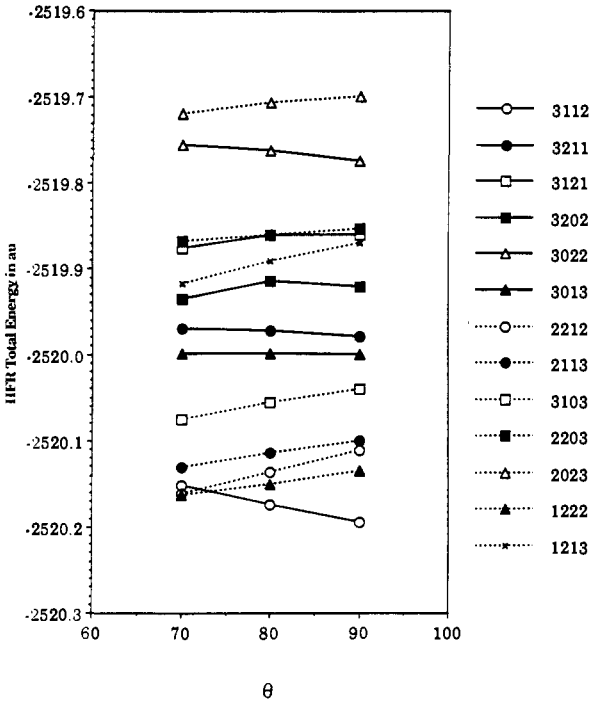

Figure 1. Plot of the HFR total energy as a function of the Mn–Mn–C bond angle, θ, for the 13 M–M electron configurations of $Mn_2(CO)_2$. Solid lines join configurations whose total energy increases from 90° to 80° (θ), while dashed lines join configurations whose total energy decreases from 90° to 80°.

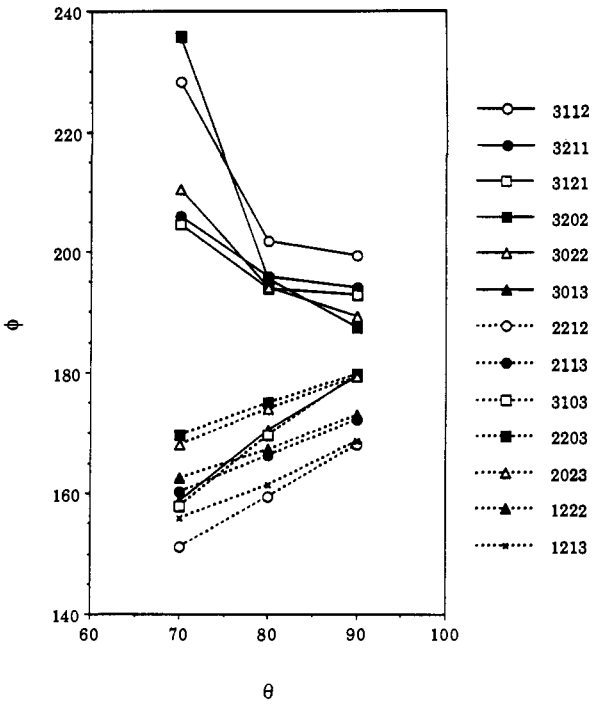

Figure 2. Plot of the Mn–C–O bond angle, ϕ, as a function of the Mn–Mn–C bond angle, θ, for each $Mn_2(CO)_2$ configuration. The line convention of Figure 1 is utilized.

expect each group to have common occupied M–M MO's, which control the behavior of the carbonyl ligand. For the $Mn_2(CO)_2$ configurations that show an increase in energy, the common MOs are three a_g and one b_u. Although the common a_g orbitals are mixtures of those in Table I, they can be resolved into σ, δ_{ip}, and π^*_{ip}; the common b_u orbital is π_{ip}. For the $Mn_2(CO)_2$ configurations that show a decrease in energy and favor a bridging carbonyl, the common MO's are one a_g and two b_u's. The a_g has $\sigma + \delta_{ip}$ character while the two b_u's have π_{ip} and $\sigma^* + \delta^*_{ip}$ character, respectively.

Generally, as θ decreases from 90° to 80° the orbital energies of $\sigma(a_g)$, $\pi_{ip}(b_u)$, and $\pi^*_{ip}(a_g)$ increase, while the orbital energies of $\delta_{ip}(a_g)$, $\delta^*_{ip}(b_u)$, and $\sigma^*(b_u)$ decrease. Thus, configurations with the former orbitals occupied favor a terminal structure, while those with more of the latter group occupied favor the bridging structure. An interesting comparison is provided by configurations 3013 and 3103. Each configuration has three a_g and three b_u MO's with the remaining M–M electron pair occupying either an a_u or a b_g M–M MO. Thus, when both the a_g and b_u MO's are occupied, the system is nearly balanced and the out-of-plane MO's (a_u and b_g) control the geometry. For 3103 the a_u M–M MO, which has π_{op} character, strongly favors the bridging position, while for 3013 the b_g, which has δ_{op} character, is less particular. The origin of this can be seen in Table I, where the $a_u(\pi_{op})$ has its maximum density along the M–M axis and the $b_g(\delta_{op})$ has its maximum density facing the terminal carbonyl sites. Since these are the only out-of-plane orbitals occupied, their character has a strong influence on the position of the CO if it is to use its $2\pi_{op}$ orbital in metal–ligand bonding.

Figure 2 shows the Mn–C–O bond angle, ϕ, as a function of θ for all of the $Mn_2(CO)_2$ configurations. The $Mn_2(CO)_2$ configurations which favor terminal carbonyls (solid lines), except 3013, have a large increase in ϕ, i.e. a linear or prone semibridging carbonyl, when the carbonyl is forced to adopt a bridging position (smaller θ). Configuration 3013 favors a small value of ϕ because the b_g M–M MO with δ_{op} character, the same MO that favors a terminal carbonyl (see preceding paragraph), can maximize its bonding interaction with the carbonyl ligand only if ϕ decreases as θ decreases. All of the $Mn_2(CO)_2$ configurations that favor bridging carbonyls (dashed lines) show a decrease in ϕ when θ is decreased, i.e. a bent semibridging or symmetric bridging carbonyl. *Thus, no configurations that energetically favor a bridging carbonyl adopt the linear semibridging conformation, 4.*

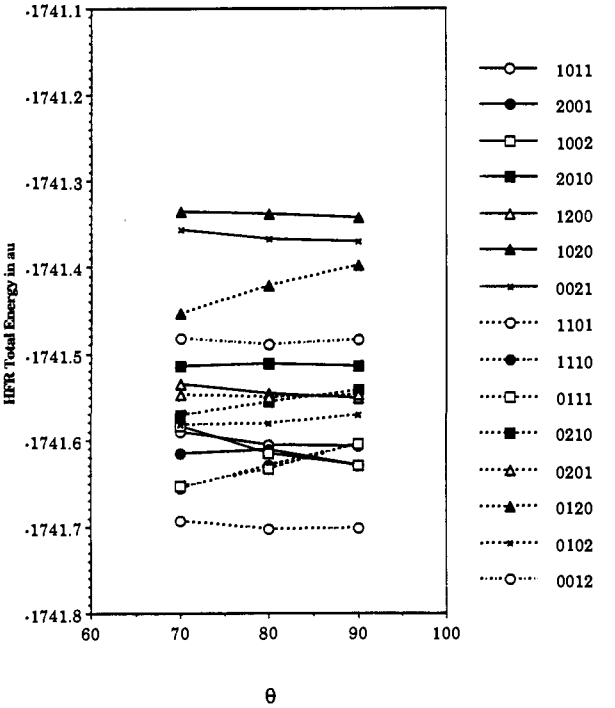

Figure 3. Plot of the HFR total energy as a function of the Sc–Sc–C bond angle, θ, for the 15 configurations of $Sc_2(CO)_2$. Solid lines join configurations whose total energy increases from 90° to 80° (θ), while dashed lines join configurations whose total energy decreases from 90° to 80°.

Results for M = Sc. Figure 3 illustrates the behavior of the HFR total energy for the $Sc_2(CO)_2$ configurations as a function of θ. Seven of the $Sc_2(CO)_2$ configurations—1011, 2001, 1002, 2010, 1200, 1020, 0021—increase in energy, i.e. favor a terminal carbonyl, while the remaining eight—1101, 1110, 0111, 0210,

Chart I

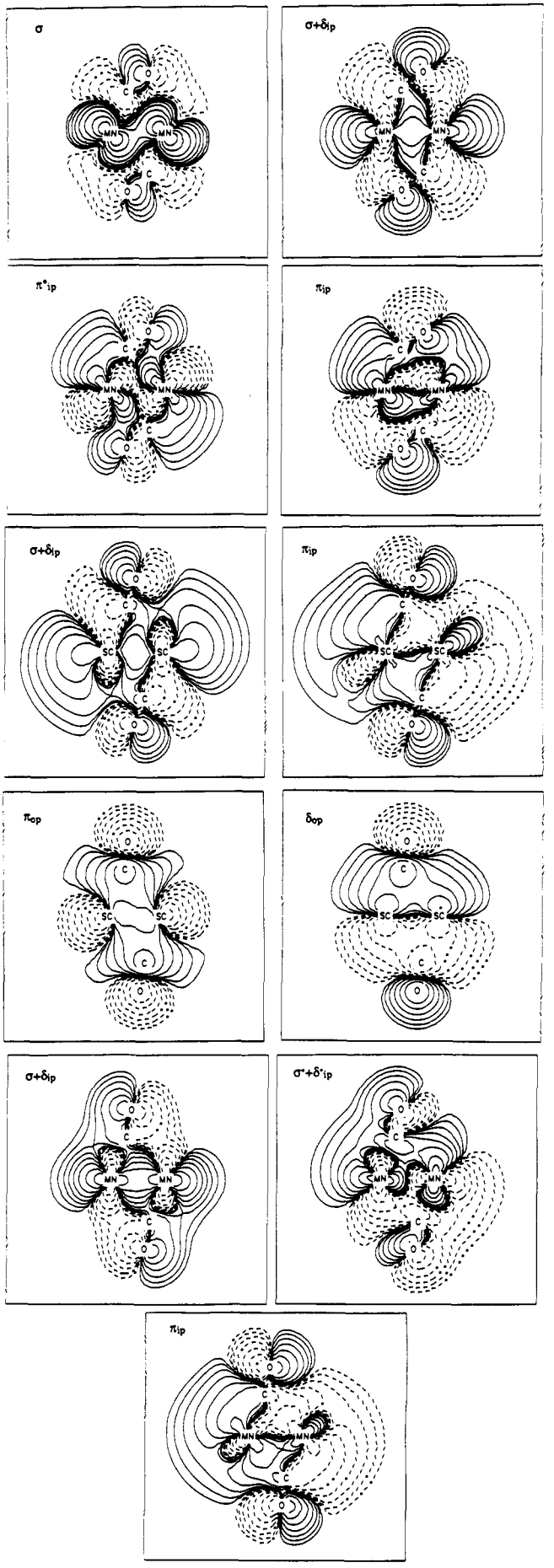

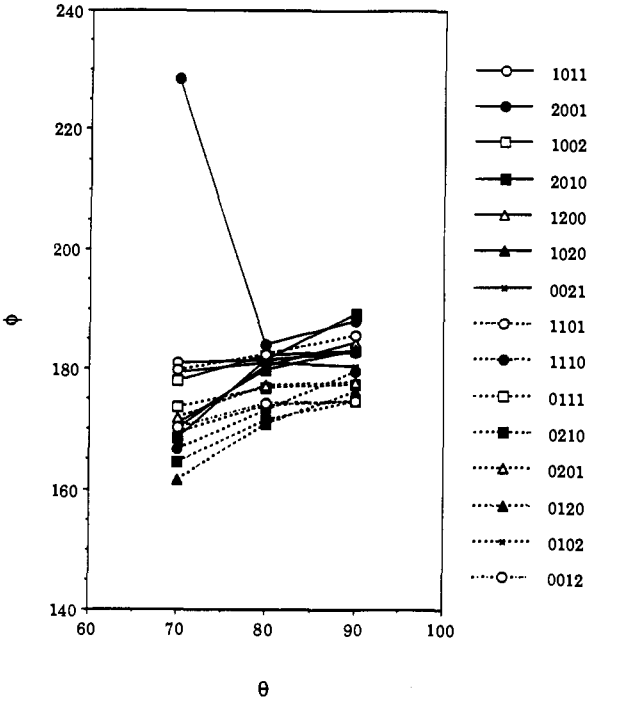

Figure 4. Plot of the Sc–C–O bond angle, ϕ, as a function of the Sc–Sc–C bond angle, θ, for each $Sc_2(CO)_2$ configuration. The line convention of Figure 3 is utilized.

0201, 0120, 0102, 0012—decrease in energy, i.e. favor a bridging carbonyl.

As was true for the $Mn_2(CO)_2$ configurations, the two groups of $Sc_2(CO)_2$ configurations have common sets of M–M MO's. The $Sc_2(CO)_2$ configurations, which favor a terminal carbonyl, have at least one a_g and/or one b_u M–M MO, while the $Sc_2(CO)_2$ configurations, which favor the bridging carbonyl, have at least one a_u and/or one b_g M–M MO. The largest energy increases occur for those configurations that have only a_g and b_u MO's (in-plane) occupied, while the largest energy decreases occur for those configurations that have both a_u and b_g MO's (out-of-plane) occupied. For the $Sc_2(MO)_2$ configurations favoring terminal carbonyls, the common a_g and b_u M–M MO's have $\sigma + \delta_{ip}$ and π_{ip} character, respectively, while for those $Sc_2(CO)_2$ configurations favoring a bridging carbonyl, the common a_u and b_g M–M MOs have π_{op} and δ_{op} character, respectively.

As for $Mn_2(CO)_2$, the $\sigma(a_g)$ and $\pi_{ip}(b_u)$ MO's generally favor the terminal carbonyls, while the $\pi_{op}(a_u)$ and $\delta_{op}(b_g)$ generally favor bridging carbonyls. Figure 4 illustrates the Sc–C–O bond angle, ϕ as a function of θ. At $\theta = 80°$ all of the configurations favoring terminal carbonyls (solid lines) have essentially linear semibridging carbonyls. On the other hand, the $Sc_2(CO)_2$ configurations favoring bridging carbonyls (dashed lines) all have bent semibridging carbonyls as θ decreases from 90°. The $Sc_2(CO)_2$ configurations 1101 and 2010 appear to be the most severe exceptions. However, these two configurations are also capricious in the behavior of their total energy (Figure 3), which decreases (increases) from 90° to 80° and then increases (decreases) from 80° to 70°, respectively. If we confine ourselves to those configurations whose energy change is most dramatic, the results for $Sc_2(CO)_2$ clearly parallel those of $Mn_2(CO)_2$.

Conclusions

For both systems, we have found no configurations that favor a bridging geometry and adopt a linear semibridging conformation. Only those configurations that favor a terminal carbonyl and are then forced into a bridging position adopt a linear semibridging conformation. Therefore, linear semibridging carbonyls in homonuclear dimers are a consequence of steric crowding.

The configurations that favor terminal carbonyls and, hence, linear semibridging carbonyls have common M–M MO's with σ, δ_{ip}, π_{ip}, and π^*_{ip} character. Thus, linear semibridging confor-

mations are characterized by configurations with a high bond order and few occupied antibonding M-M MO's. Those $Mn_2(CO)_2$ configurations that favor a bridging carbonyl have common M-M MO's with σ, δ_{ip}, σ^*, δ^*_{ip}, and π_{ip} character. Generally, when these $Mn_2(CO)_2$ configurations have more than one a_g and more than two b_u M-M MO's occupied, the extra a_g and b_u M-M MO's have π^*_{ip} and σ^* character, respectively. Thus, bent semibridging and symmetrically bridging conformations are characterized by configurations with a low bond order. The appearance of linear semibridging signifies strong metal-to-metal bonding.

In the previous work of Hall et al.[9a] and Benard et al.[1c] on linear semibridging carbonyls, linear semibridging was attributed to the maximization of the interaction between an occupied in-phase combination of metal d orbitals and one lobe of the carbonyl 2π orbital. Although orbital interactions like those previously described[9,10] exist here, they are not the primary origin of the observed structure. In many cases, these interactions may be a response to the linear semibridging structure forced upon the system by steric considerations. Thus, in this electronic interaction the system is attempting to minimize the repulsive interactions by creating an in-phase orbital combination.

In real compounds, as opposed to our simple $M_2(CO)_2$ model, it is much more difficult to resolve the competing effects of steric (repulsive) and bonding (attractive) interactions. The observed equilibrium geometry is, of course, a balance of both, and any distortions from this structure affect both interactions. In addition, both interactions are electronic in origin and cannot be separated in any rigorous way. Thus, the structure of a dimer is determined by inter- and intrafragment electronic effects (both steric and bonding) and one cannot predict from our model alone how a change in a non-bridging ligand or a change in the metal might modify the structure.

Acknowledgment. The authors wish to thank the National Science Foundation (Grant No. CHE 86-19420 and CHE 91-13634) and the Robert A. Welch Foundation (Grant No. A-648) for financial support, M. F. Guest for use of the program GAMESS, SERC Daresbury Laboratory, Warrington, WA4 4AD, U.K., and P. Sherwood and P. J. MacDougall for interactive MOPLOT. This research was conducted in part with the use of the Cornell National Supercomputer Facility, a resource for the Center for Theory and Simulation in Science and Engineering at Cornell University, which is funded in part by the National Science Foundation, New York State, and the IBM Corp., and in part at the Texas A&M University Supercomputer Center with a grant from Gray Research Inc.

Registry No. $Sc_2(CO)_2$, 138355-11-0; $Mn_2(CO)_2$, 54822-31-0.

Solvent Effects. 3. Tautomeric Equilibria of Formamide and 2-Pyridone in the Gas Phase and Solution. An ab Initio SCRF Study

Ming Wah Wong,[†] Kenneth B. Wiberg,*[,†] and Michael J. Frisch[‡]

Contribution from the Department of Chemistry, Yale University, New Haven, Connecticut 06511, and Lorentzian Inc., 127 Washington Avenue, North Haven, Connecticut 06473.
Received August 5, 1991

Abstract: High level ab initio molecular orbital studies, using basis sets up to 6-31+G**, with electron correlation included at the second-order Møller-Plesset perturbation (MP2) and quadratic configuration interaction with singles and doubles (QCISD) levels, are reported for the tautomeric equilibria of formamide/formamidic acid and 2-pyridone/2-hydroxypyridine in the gas phase and solution. The solvent effects on the tautomeric equilibria were investigated by self-consistent reaction field (SCRF) theory. The calculated tautomerism free energy changes for 2-pyridone in the gas phase, cyclohexane, and acetonitrile are -0.64, 0.36, and 2.32 kcal mol^{-1}, in very good agreement with the experimental values (-0.81, 0.33, and 2.96 kcal mol^{-1}, respectively). The introduction of a dielectric medium has little effect on the electronic structure of the enol forms. On the other hand, significant effects on the molecular geometry, charge distributions, and vibrational frequencies are found for the more polar keto tautomers. The calculated changes are readily understood in terms of the increasing weight of the dipolar resonance structure.

Introduction

The 2-pyridone/2-hydroxypyridine equilibrium represents one of the classic cases of medium-dependent tautomeric equilibrium.[1] In the gas phase, the preference of the hydroxy-form has been conclusively shown by IR, UV, mass spectrometric, and photoelectron experiments.[2] In nonpolar solvents such as cyclohexane, both tautomers exist in comparable amounts.[3] However, in solvents of high dielectric constant[3] and in the solid state,[4] the tautomeric equilibrium is shifted in favor of the more polar oxo-form. The dependence of such an equilibrium constant on solvent polarity has been reported previously by Frank and Katritzky[3a] and by Kuzuya et al.[3b] The theoretical prediction of the tautomerism energy of 2-pyridone has been the subject of intense interest in the past decade.[1d,5] Most ab initio calculations to date have focused on the relative stability of the two tautomeric forms

[†] Yale University.
[‡] Lorentzian Inc.

(1) (a) Katritzky, A. R.; Lagowski, J. M. *Adv. Heterocycl. Chem.* **1963**, *1*, 339. (b) Kwiatkowski, J. S.; Pullman, B. *Adv. Heterocycl. Chem.* **1975**, *18*, 199. (c) Pullman, B.; Pullman, B. *Adv. Heterocycl. Chem.* **1975**, *18*, 199. (d) Kwiatkowski, J. S.; Zielinski, T. J.; Rein, R. *Adv. Quantum Chem.* **1986**, *18*, 85.

(2) (a) Beak, P.; Fry, F. S. *J. Am. Chem. Soc.* **1973**, *95*, 1700. (b) Beak, P.; Fry, F. S., Jr.; Lee, J.; Steele, F. *J. Am. Chem. Soc.* **1976**, *98*, 171. (c) Beak, P. *Acc. Chem. Res.* **1977**, *10*, 186. (d) Nowak, M. J.; Sczepaniak, K.; Barski, A.; Shugar, D. *Z. Naturforsch.* **1978**, *33C*, 876. (e) Aue, D. H.; Betowski, L. D.; Davidson, W. R.; Bowers, M. T.; Beak, P.; Lee, J. *J. Am. Chem. Soc.* **1980**, *102*, 1174. (f) Brown, R. S.; Tse, A.; Vederas, J. C. *J. Am. Chem. Soc.* **1980**, *102*, 1174. (g) Nimlos, M. R.; Kelley, D. F.; Bernstein, E. R. *J. Phys. Chem.* **1989**, *93*, 643.

(3) (a) Frank, J.; Katritzky, A. R. *J. Chem. Soc., Perkin Trans. II* **1976**, 1428. (b) Kuzuya, M.; Noguchi, A.; Okuda, T. *J. Chem. Soc., Perkin Trans. II* **1985**, 1423.

0002-7863/92/1514-1645$03.00/0 © 1992 American Chemical Society